Cancer Letters 485 (2020) 27–37

Contents lists available at ScienceDirect

Cancer Letters

journal homepage: www.elsevier.com/locate/canlet

IMPAD1 functions as mitochondrial electron transport inhibitor that prevents ROS production and promotes lung cancer metastasis through the AMPK-Notch1-HEY1 pathway

Yi-Fang Yang[a,b,1], Yen-Yun Wang[b,c], Michael Hsiao[d,e], Steven Lo[f], Yu-Chan Chang[d], Yi-Hua Jan[d], Tsung-Ching Lai[d], Yi-Chen Lee[g], Ya-Ching Hsieh[h], Shyng-Shiou F. Yuan[a,b,i,j,*]

[a] Translational Research Center, Kaohsiung Medical University Hospital, Kaohsiung Medical University, Kaohsiung, Taiwan
[b] Center for Cancer Research, Kaohsiung Medical University, Kaohsiung, Taiwan
[c] School of Dentistry, College of Dental Medicine, Kaohsiung Medical University, Kaohsiung, Taiwan
[d] Genomics Research Center, Academia Sinica, Taipei, Taiwan
[e] Department of Biochemistry, College of Medicine, Kaohsiung Medical University, Kaohsiung, Taiwan
[f] College of Medical, Veterinary and Life Sciences, University of Glasgow, Glasgow, UK
[g] Department of Anatomy, School of Medicine, College of Medicine, Kaohsiung Medical University, Kaohsiung, Taiwan
[h] Institute of Cancer Sciences, University of Glasgow, Glasgow, UK
[i] Department of Medical Research and Department of Obstetrics and Gynecology, Kaohsiung Medical University Hospital, Kaohsiung Medical University, Kaohsiung, Taiwan
[j] Graduate Institute of Medicine, College of Medicine, Kaohsiung Medical University, Kaohsiung, Taiwan

ARTICLE INFO

Keywords:
IMPAD1
Lung cancer
AMP
Metabolism
Tumor microenvironment
ADORA1

ABSTRACT

The tumor microenvironment (TME) and metabolic reprogramming have been implicated in cancer development and progression. However, the link between TME, metabolism, and cancer progression in lung cancer is unclear. In the present study, we identified IMPAD1 from the conditioned medium of highly invasive CL1-5. High expression of IMPAD1 was associated with a poorer clinical phenotype in lung cancer patients, with reduced survival and increased lymph node metastasis. Knockdown of IMPAD1 significantly inhibited migration/invasion abilities and metastasis *in vitro* and *in vivo*. Upregulation of IMPAD1 and subsequent accumulation of AMP in cells increased the pAMPK, leading to Notch1 and HEY1 upregulation. As AMP is an ADORA1 agonist, treatment with ADORA1 inhibitor reduced the expression of pAMPK and HEY1 expression in IMPAD1-overexpressing cells. IMPAD1 caused mitochondria dysfunction by inhibiting mitochondrial Complex I activity, which reduced mitochondrial ROS levels and activated the AMPK-HEY1 pathway. Collectively this study supports the multipotent role of IMPAD1 in promotion of lung cancer metastasis by simultaneously increasing AMP levels, inhibition of Complex I activity to decrease ROS levels, thereby activating AMPK-Notch1-HEY1 signaling, and providing an alternative metabolic pathway in energy stress conditions.

1. Introduction

Lung cancer is one of the most common malignancies in Taiwan and remains the leading cause of cancer-related death globally, with more than 1.3 million people dying of the disease annually [1]. Non–small-cell lung carcinoma (NSCLC) cases account for approximately 80% of all lung cancer cases [2,3]. Approximately 70% of all newly diagnosed NSCLC patients exhibit locally advanced or metastatic disease and require systemic treatment. NSCLC patients often have a poor prognosis, and the 5-year survival rate of patients at all stages combined is only 15% [3–5], concomitant with its high rate of metastasis [6].

The tumor microenvironment (TME) - including stromal-derived enzymes, secretory proteins, and cytokines - drives the malignant phenotype of cancer cells [7]. In recent years, focus has shifted in particular to the secretome and the critical role that this plays in the malignant phenotype of lung cancer cells [8,9]. The secretome refers to the library of proteins that are released from cells, tissue, or organism through different mechanisms, including classical secretion, non-classical secretion, membrane protein shedding, and exosomal secretion [10–12]. Tumor progression to metastasis involves specific molecular

* Corresponding author. Translational Research Center, Kaohsiung Medical University Hospital, Kaohsiung Medical University, 100 Zihyou 1st Road, San-Ming District, Kaohsiung, Taiwan.
E-mail address: yuanssf@ms33.hinet.net (S.-S.F. Yuan).
[1] Current address: Department of Medical Education and Research, Kaohsiung Veterans General Hospital, Kaohsiung, Taiwan.

https://doi.org/10.1016/j.canlet.2020.04.025
Received 19 February 2020; Received in revised form 8 April 2020; Accepted 28 April 2020

interactions between cancer cells and the surrounding extracellular matrix; however, how cancer cells regulate these molecular interactions is not clearly defined [7]. Metabolic reprogramming - vital to cancer cell survival under energy stress conditions, including anchorage-independent growth and solid tumor formation [13] – may additionally play a role in such cancer cell and extracellular matrix interactions. Aside from their role in energy production, mitochondria produce cellular reactive oxygen species (ROS) that play a role in cellular signaling [14,15], with modification of cellular physiology and molecular signaling by regulation of ROS concentration [16]. In this regard, cancer cells may increase antioxidant levels to maintain homeostasis, while chemotherapeutic drugs may kill cancer cells by increasing ROS levels. Alternatively, targeting antioxidants may cause cancer cells to produce ROS [17,18].

In order to answer some of these critical questions regarding tumor microenvironment and metabolic reprogramming, we therefore specifically focused on proteins relevant to cancer metabolism in the secreted proteins differentially expressed in lung cancer cells. This highlighted the potential role of inositol monophosphatase domain-containing 1 (IMPAD1), the enzyme responsible for the hydrolysis of phosphoadenosine phosphate (PAP) to adenosine monophosphate (AMP), in lung tumor metastasis and migration. Other than its location in Golgi [32], IMPAD1 is also identified from the exosome isolated from the conditioned medium of CL1-5 lung cancer cells [8]. In this study we explored both a novel metastasis promoting pathway involving IMPAD1-AMPK-Notch1-Hey1, and a potential alternative metabolic pathway to AMPK activation in NSCLC.

2. Materials and methods

2.1. Cell lines and conditioned medium

CL1-0, CL1-5, H441, and H460 lung cancer cell lines were cultured in RPMI-1640 medium containing 10% FBS and 1% PSG. The H1299 cell line was maintained in DMEM containing 10% FBS and 1% PSG. For preparing CM, CL1-0 and CL1-5 lung cancer cell lines were plated at 3×10^5 cells/well in a 6-well plate and were incubated for 24 h at 37 °C. After 24 h, the cells were washed with serum-free medium (SFM) and incubated in SFM for 24 h at 37 °C. On the next day, CM was collected into Ultra-15 tubes (molecular weight cut-off: 3 kDa; Millipore, Billerica, MA, USA). The BCA assay (Pierce™ BCA Protein Assay Kit; Thermo Fisher, IL, USA) was used to determine the protein concentration.

2.2. Immunoblotting

Proteins were extracted using RIPA buffer, and the protein concentration was measured using the BCA protein assay kit (Pierce™ BCA Protein Assay Kit; Thermo Fisher, IL, USA). Proteins from cell lines or CM were loaded onto SDE-PAGE gel (10%). After being transferred to a PVDF membrane, blocking with 5% BSA in TBST was conducted. The antibodies and condition are listed in Supplemental Table S4.

2.3. Lentiviral infection

Lentiviral particles of IMPAD1 were purchased from GeneCopoeia (#W1522, MD, USA). Viral supernatants of IMPAD1, HEY1, and Notch1 shRNA were purchased from the National RNAi Core Facility Platform (Taipei, Taiwan; target sequences are provided in Table S4). Viral supernatants were used to infect lung cancer cells in complete medium containing 8 μg/mL polybrene. After 72 h, the cells were selected using 2 μg/mL puromycin.

2.4. Online data analysis

We used a publicly available lung cancer microarray to construct the overall survival curve using the Kaplan–Meier method; the curve was stratified according to the expression of *IMPAD1* and *ADORA1* (http://kmplot.com/analysis/index.php?p=service&cancer=lung) [19]. PrognoScan is a microarray database that presents the hazard ratio by statistical expression of target genes and survival in patient samples (http://dna00.bio.kyutech.ac.jp/PrognoScan/). The IHC staining results of normal tissues and cancer tissues were obtained from the HPA (https://www.proteinatlas.org/).

2.5. Cell migration/invasion assay

Migration and invasion assays were performed using transwell chambers, as previously described [20]. In brief, the cells were re-suspended in SFM (2×10^5 cells/mL) and loaded into transwell chambers (upper chamber) in 100 μL. After 24 h, the cells were stained by crystal violet and were counted (bottom chamber) under a microscope. For the conditioned medium experiments, CL1-0 and H441 cells were pretreated with the conditioned medium (CM) from IMPAD1-overexpressing or IMPAD1-knockdowned CL1-5 cells for 48 h. Then, the cells were trypsinized for the transwell cell migration and invasion assays.

2.6. Animal studies

Animal experiments were conducted in accordance to the protocol approved by the Animal Care and Use Committee of Kaohsiung Medical University and Academia Sinica Institutional Animal Care. BALB/cAnN.Cg-Foxn1nu/CrlNarl (immunodeficient mice) male mice were used. For *in vivo* metastasis assay, CL1-5/shluc and CL1-5/shIMPAD1 cells were resuspended in PBS (1×10^6 cells/0.1 mL) and injected into the tail vein of each group. For *in vivo* IMPAD1 overexpression model, H441/Vector and H441/IMPAD1 cells were used 6-week-old nonobese, diabetic, severe-combined immunodeficient (NOD-SCID) male mice. At the end point, sections underwent H&E staining, and metastatic nodules were then quantified under a microscope. For orthotopic metastasis assay, the cells were resuspended in PBS and mixed with GFR-Matrigel (BD Labware) (1:1); metastatic lung nodules were quantified using a microscope.

2.7. AMP assay

The cells were plated at a density of 1×10^4 cells per well in 96-well plates in complete medium and were incubated overnight at 37 °C in 5% CO_2. Following incubation, medium was replaced for each cell line, which was incubated for 1 h. Moreover, 25 μL from each well was transferred to a solid white plate. For AMP detection, the AMP-GloTM assay (Promega, #V5011) was performed.

2.8. AMP replenishment

CL1-5/shluc and CL1-5/shIMPAD1 cells were plated at 3×10^5 in a 6-well plate in complete medium and were incubated overnight at 37 °C in 5% CO_2. On the next day, the cells were washed with complete medium and treated with or without adenosine 5′-monophosphate monohydrate (Sigma-Aldrich, #A2252, 38 nM) in complete medium.

2.9. ROS quantification

To evaluate cytoplasmic ROS, the cells were plated in a 6-well plate (3×10^5) and were incubated overnight at 37 °C in 5% CO_2. Subsequently, the cells were incubated with 2′7′-dichlorodihydrofluorescein diacetate (DCFDA, 10 μM; Sigma-Aldrich, #D6883) for 20 min. Following the removal of DCFDA, the cells were resuspended in PBS and analyzed through flow cytometry (Beckman Coulter Cytomics FC500). To determine mitochondrial ROS, the cells were incubated in MitoSOX (10 μM; Thermo Fisher Scientific, #M36008).

2.10. Oxygen consumption rate and extracellular consumption rate

The OCR and ECAR were measured using an XF^e-24 Analyzer (Seahorse Bioscience). For the OCR assay, stable cell lines were treated with or without 1 μM oligomycin, 0.5 μM carbonyl cyanide-p-trifluoromethoxyphenylhydrazone (FCCP), 0.5 μM rotenone, and 0.5 μM antimycin A (XF cell mito stress test kit, Seahorse Bioscience). For the ECAR assay, stable cell lines were treated with or without 10 mM glucose, 1 μM oligomycin, 0.5 μM rotenone, and 50 mM 2-deoxy-D-glucose (2-DG) (XF glycolysis stress test kit, Seahorse Bioscience).

2.11. Complex I and complex III activity assay

Stable cell lines were plated in a 10-cm dish (5×10^6) in complete medium at 37 °C for 24 h. On the next day, the cells were washed with PBS, and mitochondria were then extracted using a mitochondria isolation kit (#K228-50, BioVison). Complex I activity and Complex III activity were determined using the Mitochondrial Complex I Activity Colorimetric Assay Kit (#K968-100, BioVison) and Mitochondrial Complex III Activity Assay Kit (#K520-100, BioVison). The results were normalized to the protein concentration.

2.12. Statistical analysis

All statistical analyses were performed using SPSS software (Statistical Package for the Social Sciences, version 19.0). Data are presented as the mean ± SD, and data were analyzed using the two-tailed Student *t*-test. Clinicopathological characteristics were compared using the chi-square test. Correlations between parameters were analyzed using Spearman's correlation. $P < 0.05$ was considered significant.

3. Results

3.1. Identification of IMPAD1 in the highly invasive CL1-5 cell line

To identify secretomic proteins associated with lung cancer invasion, we analyzed proteins that were differentially expressed in conditioned media between noninvasive CL1-0 lung cancer cells and their relatively highly invasive counterpart CL1-5 cells [8] (Fig. 1A). We identified that 15 proteins, putatively associated with lung cancer invasion, were significantly enriched in the conditioned media of highly invasive CL1-5 cells (Supplementary Table 1). Based on the Human Protein Atlas (HPA) database (score > 2) and cDNA microarray database (Kaplan–Meier Plotter and PrognoScan), we selected IMPAD1 for further investigation (Supplementary Table 1). IMPAD1 was upregulated in highly invasive CL1-5 cells, including in the conditioned medium (CM) and cell extract (CE) (Fig. 1B and C). Moreover, RNA levels of *IMPAD1* were upregulated in CL1-5 and lung cancer tissues, and *IMPAD1* expression was associated with poor survival, as revealed by a publicly available lung cancer microarray (GSE7670 and GSE31210) and Kaplan–Meier survival analyses (Fig. 1D, F). We also examined the protein levels of IMPAD1 in lung cancer patients by using our lung cancer tissue array. Analysis of IMPAD1 expression was based on the immunopositive staining of cytoplasmic IMPAD1 (Fig. 1G). Using clarified expression criteria, we classified patients into an IMPAD1-low group and an IMPAD1-high group (> 10%). The data showed that high levels of IMPAD1 expression in lung cancer patients was significantly associated with lymph node metastasis ($P = 0.012$) (Supplementary Table 2). This result suggests that IMPAD1 is associated with lung cancer progression.

3.2. Overexpression of IMPAD1 promotes lung cancer invasion and metastasis

Our clinical findings suggest that IMPAD1 plays a role in lung cancer progression. We investigated the effects of IMPAD1 perturbation phenotype on invasion, migration, and proliferation abilities of lung cancer cells. Endogenous IMPAD1 was upregulated in highly invasive lung cancer cells CL1-5 and H1299 (Fig. 2A), and IMPAD1 knockdown significantly reduced their migration/invasion abilities (Fig. 2B, Supplementary Figs. 1A and C). Conversely, IMPAD1 overexpression significantly increased migration/invasion in less invasive CL1-0 and H441 lung cancer cell lines (Fig. 2C, Supplementary Figs. 1B and D). Cell proliferation was not altered by knockdown or overexpression of IMPAD1 in lung cancer cells (Supplementary Fig. 1E). We also examined the effect of the conditioned medium (CM) of CL1-5 cells with high IMPAD1 expression on the migration and invasion potential of CL1-0 and H441 cells. We pretreated CL1-0 and H441 cells with CM from CL1-5 and CL1-5/shIMPAD1 cells and found that CM of CL1-5 promoted the migration/invasion abilities of CL1-0 and H441 cells, which were suppressed by the CM of CL1-5/shIMPAD1 (Supplementary Fig. 2A). Moreover, replenishment of IMPAD1 recombinant protein in CM of CL1-5/shIMPAD1 cells restored the migration ability of CL1-0 and H441 cells (Supplementary Fig. 2B).

To further evaluate the effects of IMPAD1 on metastasis *in vivo*, we intravenously (i.v.) injected IMPAD1-knockdown CL1-5 cells into the lateral tail vein of mice. IMPAD1 knockdown resulted in reduced lung metastases compared with controls (shluc) (Fig. 2D). We also quantified the grade of lymph node invasion by scoring the levels of cytokeratin 18 (CK18) [21,22]. Compared with control (shluc), knockdown of IMPAD1 reduced CK18 expression in mouse lymph nodes (Fig. 2E). In a comparative experiment, IMPAD1 overexpression in H441 lung cancer cells on metastasis was analyzed after i.v. injection and orthotopic (left lung) implantation into mice. In the tail vein model, IMPAD1 overexpression increased the number of metastatic lung foci (Fig. 2F). Moreover, similar results were obtained for the orthotopic model, in which increased numbers of metastatic lung foci were found in the right lung of mice injected with the primary tumors formed in the left lung (Fig. 2G).

3.3. Upregulated IMPAD1 enhances Notch1-Mediated signaling and HEY1 expression

To identify the potential molecular mechanisms of IMPAD1, we used gene expression RT^2 profiler PCR arrays to examine control cells (CL1-5/shluc) and IMPAD1-knockdown CL1-5 cells. Knockdown of IMPAD1 resulted in the downregulation of the Notch1 pathway (Fig. 3A, Supplementary Figs. 3A and B and Table 3). Furthermore, the RNA level of Hes-Related Family BHLH Transcription Factor With YRPW Motif 1 (HEY1), which is involved in the epithelial–mesenchymal transition (EMT) process [23], showed the highest downregulation in IMPAD1-knockdown cells (Fig. 3A). Western blotting and real-time PCR also demonstrated that HEY1 expression was significantly downregulated after IMPAD1 knockdown (Fig. 3B, Supplementary Fig. 3C). Conversely, Western blotting confirmed that HEY1 was upregulated in IMPAD1-overexpressing CL1-0 and H441 cells compared with vector control cells (Fig. 3C). We therefore validated that IMPAD1 promoted the migration and invasion abilities of lung cancer cells through HEY1. As shown in Fig. 3D, migration and invasion abilities were significantly inhibited in IMPAD1-overexpressing cells through HEY1 suppression. These data suggest that IMPAD1 promotes invasion through HEY1. Since HEY1 expression increases and accumulation in the nucleus are regulated by Notch signaling [24,25], we determined whether IMPAD1 activates Notch1. Indeed, the Notch signaling reporter assay demonstrated that Notch activity was significantly upregulated after IMPAD1 overexpression (Supplementary Fig. 3D). In IMPAD1-overexpressing cells, migration and invasion abilities were significantly inhibited through the suppression of Notch1 by using shRNA or a γ-secretase inhibitor (DAPT) (Fig. 3E and F and Supplementary Figs. 3E and F). We next investigated whether IMPAD1 expression is correlated with HEY1 expression in lung cancer patients by immunohistochemistry (IHC). IHC staining for IMPAD1 and HEY1

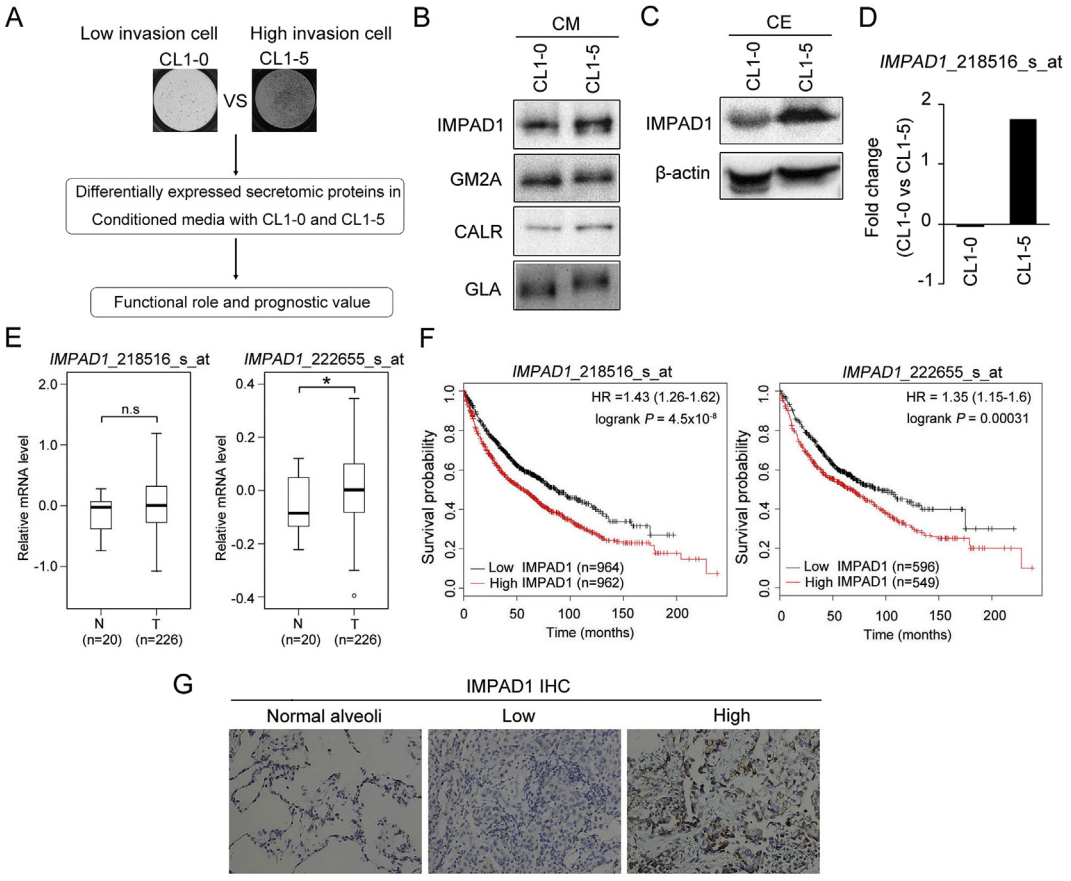

Fig. 1. Identification of IMPAD1 as a Potential Target for Lung Cancer Progression. (A) Schematic of secretomic protein screening in the conditioned medium of CL1-0 and CL1-5 cells using a proteomic dataset. (B–C), Western blot analysis of IMPAD1 protein levels secreted into conditioned media (CM) (B) and cell extract (CE) (C) from CL1-5 and CL1-0 cells. GLA, CALR, and β-actin were used as loading controls for CM and CE, respectively. (D) Relative *IMPAD1* (218516_s_at) mRNA levels in CL1-0 and CL1-5 lung cancer cells (NCBI/GEO/GSE7670). (E) Relative *IMPAD1* (218516_s_at and 222655_s_at) mRNA levels in lung adenocarcinoma tissues (NCBI/GEO/GSE31210). N = normal tissues, T = tumor tissues, and n = number of specimens. Data are presented as the mean ± SD; $^*P < 0.05$. ns, not significant. (F) The Kaplan–Meier overall survival curve constructed using publicly available lung cancer microarray datasets and stratified according to *IMPAD1* expression. (G) Representative images of IMPAD1 expression in lung adenocarcinoma tissues.

showed that IMPAD1 expression was positively correlated with HEY1 expression in the lung cancer tissues (Spearman nonparametric correlation test; correlation coefficient = 0.262; $P = 0.011$; n = 77) (Fig. 3G and H). Similar results were also observed in publicly available lung cancer microarray datasets (GSE3141) (Supplementary Fig. 3G).

3.4. IMPAD1 modulates migration through the AMP-Dependent activation of AMPK

AMPK is a sensor of energy status of cells and it can sense the change ratio of AMP [26]. IMPAD1 is an enzyme responsible for the conversion of PAP into AMP. We hypothesized that upregulated IMPAD1 might increase AMP levels and activate the AMPK pathway. As expected, IMPAD1 overexpression increased AMP levels, whereas knockdown of IMPAD1 significantly reduced AMP levels (Fig. 4A and B). IMPAD1 overexpression increased the expression of pAMPK in CL1-0 and H441 cells (Fig. 4C). Conversely, knockdown of IMPAD1 in CL1-5 and H1299 cells significantly reduced the expression of pAMPK (Fig. 4D). We further investigated whether IMPAD1 promotes migration and invasion through the AMPK pathway. Indeed, treatment with BML-275 (AMPK inhibitor) significantly inhibited migration and invasion abilities in IMPAD1-overexpressing cells (Supplementary Fig. 4A).

We next studied whether IMPAD1 mediates HEY1 expression through the AMPK pathway. IMPAD1 overexpression increased the expression of Notch1 and HEY1, which was abolished by the AMPK inhibitor BML-275 (Fig. 4E and Supplementary Fig. 4B). Conversely, treatment with an AMPK activator led to Notch1 and HEY1 upregulation in IMPAD1-knockdown cells (Fig. 4F). Moreover, AMP replenishment restored migration ability and expression of pAMPK, Notch1 and HEY1 in IMPAD1-knockdown cells (Fig. 4G and Supplementary Figs. 4C and D). We next examined whether IMPAD1 expression was correlated with pAMPK in the lung cancer tissue. IHC staining results showed that the expression of IMPAD1 was positively correlated with pAMPK in lung cancer tissues (Supplementary Figs. 4E and F). These data suggest that IMPAD1 promotes lung cancer invasion and migration through the AMPK-Notch1-HEY1 signaling pathway.

3.5. IMPAD1 modulates AMPK-HEY1 signaling through AMP-Dependent activation of ADORA1 in lung cancer cells

In our study, IMPAD1 expression increased AMP levels in IMPAD1-overexpressing cells (Fig. 4A). Since AMP can activate adenosine A1 receptor (ADORA1) and its expression is related to cancer progression [27,28], we explored whether IMAPD1 regulates ADORA1 expression in lung cancer cells. IMPAD1 overexpression caused ADORA1 upregulation in CL1-0 and H441 lung cancer cells, whereas ADORA1 was significantly reduced in IMPAD1-knockdown cells (Fig. 5A and B). We further examined whether IMPAD1 mediates HEY1 expression through ADORA1 in IMPAD1-overexpressing cells. Treatment with PD116,948 (an ADORA1 antagonist) reduced the expression of pAMPK and HEY1 in IMPAD1-overexpressing cells (Fig. 5C). Moreover, treatment with L690,330 (a potent inhibitor of inositol monophosphatase) markedly

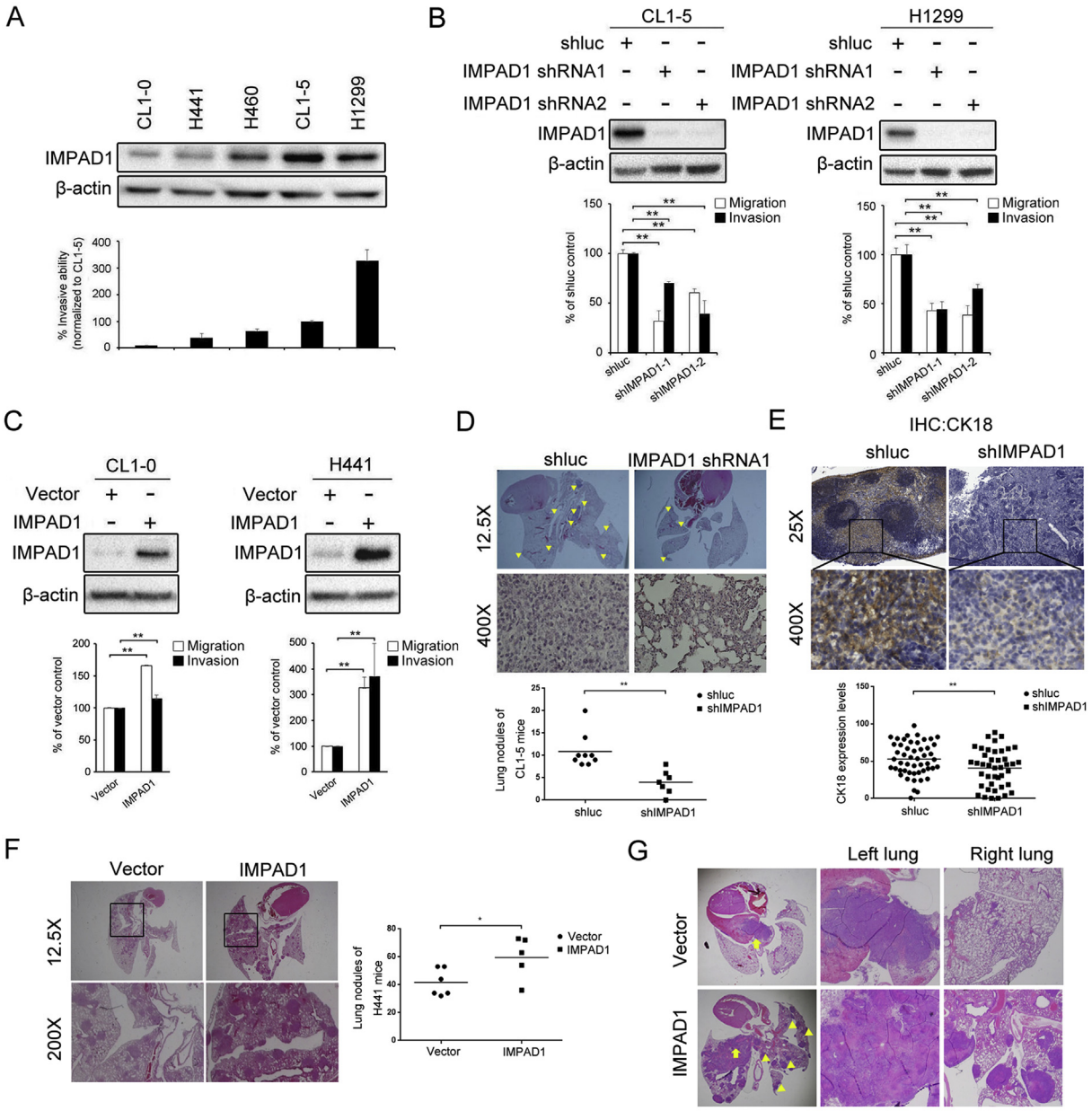

Fig. 2. IMPAD1 enhances invasion/migration and metastasis in cell and animal models. (A) Western blot analysis of endogenous IMPAD1 in lung cancer cell lines. Bottom, invasive abilities of lung cancer lines. (B) IMPAD1 knockdown and the invasion/migration abilities of CL1-5 and H1299 lung cancer cells. Top, Western blot analysis of IMPAD1 after lentiviral-mediated RNAi. Bottom, migration (open) and invasion (filled) abilities of CL1-5 cells infected with shIMPAD1 or shluc shRNA. Data are presented as the mean ± SD; $^{**}P < 0.01$. (C) Effect of IMPAD1 overexpression on migration/invasion potential of CL1-0 and H441 lung cancer cells. Top, Western blot analysis of IMPAD1 expression after IMPAD1 overexpression versus vector control treatment. Bottom, CL1-0 and H441 migration and invasion abilities after IMPAD1 overexpression. Data are presented as the mean ± SD, and significance is determined using Student's *t*-test. $^{**}P < 0.01$. (D) Top, representative image of H&E-stained lung tissues from mice intravenously injected with CL1-5-shluc or CL1-5-shIMPAD1 (n = 9). Bottom, quantification of metastatic lung nodules in individual mice 4 weeks after the tail vein was injected with CL1-5 cells after mice were infected with shluc or IMPAD1 shRNA1. Data are presented as the mean ± SD, and the significance was determined using Student's *t*-test. $^{**}P < 0.01$. (E) Representative images of CK18 expression in the lymph nodes of shluc control mice and IMPAD1-knockdown mice. Data are presented as the mean ± SD, and the significance was determined using Student's *t*-test. $^{**}P < 0.01$. (F) Tail vein model, IMPAD1 overexpression and metastasis *in vivo* in H441 cells. Left, representative image of H&E-stained lung tissues from mice intravenously injected with H441-Vector or H441-IMPAD1 cells (n = 5). Right, quantification of metastatic lung nodules in individual mice 4 weeks after the tail vein was injected with H441 cells after infection with Vector or IMPAD1. (G) Orthotopic model, IMPAD1 overexpression and metastasis *in vivo* in H441. Representative image of H&E-stained lung tissues from orthotopic mice injected with H441-Vector or H441-IMPAD1 cells (n = 4). Arrows indicate the H441/Vector or H441/IMPAD1 tumor that was established in the left lung. The arrowhead indicates metastasis nodules on the right lung.

reduced pAMPK and HEY1 expression in IMPAD1-overexpressing cells, which is similar to the effect of PD116,948 (Fig. 5D). Furthermore, Kaplan–Meier survival analyses revealed that *ADORA1* expression was associated with poor survival in lung cancer patients (Supplementary Fig. 5). Taken together, our results suggest that IMPAD1 overexpression provided AMP for activating ADORA1-AMPK signaling and increased HEY1 expression, leading to lung cancer metastasis.

3.6. IMPAD1 inhibits electron transport in lung cancer cells, resulting in decreased ROS production

AMPK can control mitochondria oxidative capacity and promote

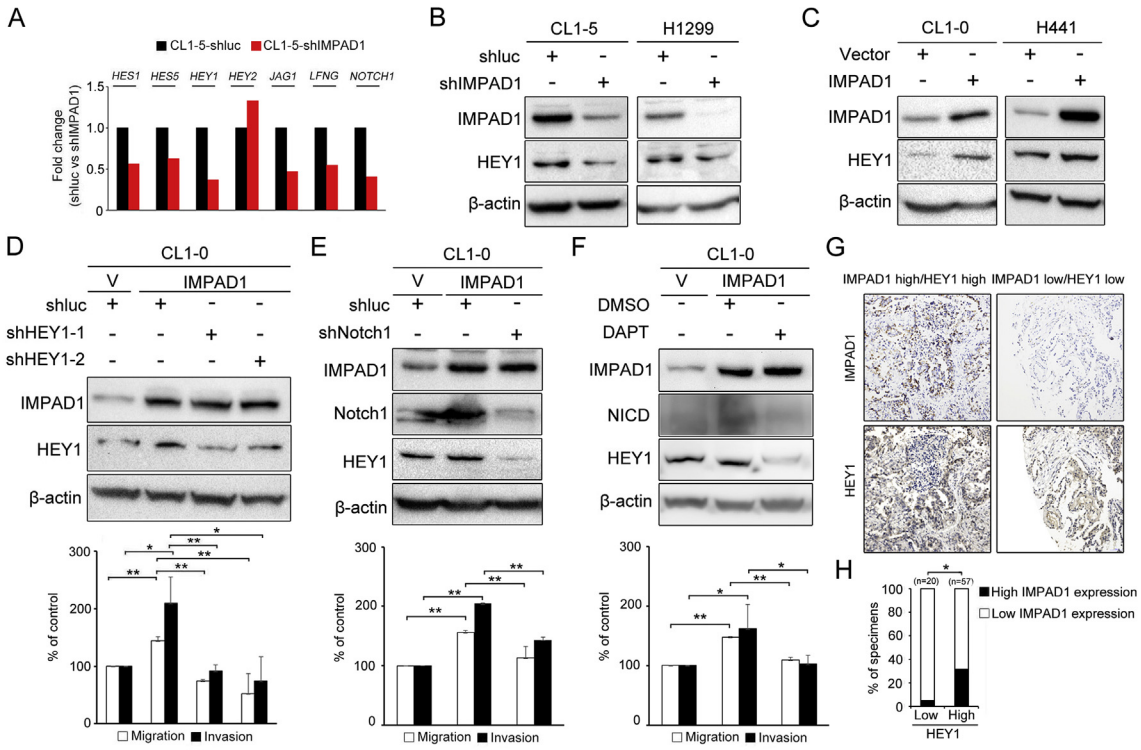

Fig. 3. IMPAD1 promotes invasion/migration through HEY1. (A) RNA levels of candidate genes relative to the shluc shRNA control. (B) Expression of IMPAD1 and HEY1 in CL1-5 and H1299 cells following IMPAD1 knockdown in comparison with the shluc shRNA control or IMPAD1 shRNA. (C) Western blot analysis of IMPAD1 and HEY1 in CL1-0/IMPAD1 and H441/IMPAD1 cells. (D) Expression of HEY1 in CL1-0 cells overexpressing IMPAD1 in comparison with the vector control. Top, Western blot analysis of IMPAD1 and HEY1 expression in CL1-0/IMPAD1 cells after HEY1 knockdown. Bottom, invasion and migration capabilities of CL1-0/IMPAD1 cells after HEY1 knockdown. Data are presented as the mean ± SD. $^{*}P < 0.05$; $^{**}P < 0.01$. (E) Top, Western blot analysis of IMPAD1, Notch1 and HEY1 expression in CL1-0/IMPAD1 cells after Notch1 knockdown. Bottom, invasion and migration capabilities of CL1-0/IMPAD1 cells after Notch1 knockdown. Data are presented as the mean ± SD. $^{*}P < 0.05$; $^{**}P < 0.01$. (F) Top, expression of IMPAD1, Notch1, and HEY1 in CL1-0/IMPAD1 cells after treatment with the γ-secretase inhibitor DAPT (10 μM). Bottom, invasion and migration capabilities of CL1-0/IMPAD1 cells after treatment with the γ-secretase inhibitor. Data are presented as the mean ± SD. $^{*}P < 0.05$; $^{**}P < 0.01$. (G) Representative IMPAD1 and HEY1 immunohistochemistry staining in a serial section of lung cancer tissue array. (H) Analysis correlation of IMPAD1 and HEY1 expression in lung cancer tissues. Data are presented as the mean ± SD. $^{*}P < 0.05$. NICD = Cleaved Notch1.

glucose uptake [29]. We evaluated whether IMPAD1 mediates the metabolic pathway in IMPAD1-overexpressing and -knockdown cells by analyzing the oxygen consumption ratio (OCR) and extracellular acidification rate (ECAR) using the Seahorse XFp Analyzer. IMPADI overexpression significantly reduced the OCR in IMPAD1-overexpressing CL1-0 cells, whereas the OCR was increased in IMPAD1-knockdown cells (Fig. 6A and B and Supplementary Fig. 6A). However, IMPAD1 expression did not affect ECAR in lung cancer cells (Supplementary Figs. 6B–D). Mitochondria is not only responsible for ATP production but also represents a source of cellular ROS [14]. To confirm the effect of IMPAD1-inhibited OCR in mitochondria on ATP and ROS production, we assessed ATP levels and ROS levels in IMPAD1-overexpressing cells. As shown in Fig. 6C and D, IMPAD1 overexpression significantly reduced ROS levels and IMPAD1 knockdown significantly increased ROS levels, whereas IMPAD1 expression did not affect ATP levels in lung cancer cells (Supplementary Fig. 6E).

We next determined whether ROS accumulation correlates with the migration and invasion abilities of lung cancer cells. H_2O_2 treatment significantly inhibited migration/invasion abilities and reduced the expression of pAMPK and HEY1 in IMPAD1-overexpressing cells (Fig. 6E). Conversely, treatment with N-acetyl-L-cysteine (NAC) (a free radical scavenger) restored the expression of pAMPK and HEY1 and migration ability in IMPAD1-knockdown cells (Fig. 6F and Supplementary Fig. 6F).

3.7. IMPAD1 inhibits ROS production through the regulation of Mitochondrial Complex I

To determine whether mitochondrial ROS production was increased in IMPAD1-knockdown cells, we analyzed ROS levels by using MitoSOXRed. Results showed that mitochondrial ROS was increased in IMPAD1-knockdown cells, whereas IMPDA1 overexpression reduced mitochondrial ROS (Fig. 7A and B). In mitochondria, Complex I and Complex III are ROS-producing systems [30]. To further examine their effect, we measured Complex I and Complex III activity in mitochondria and isolated them from IMPAD1-knockdown cells. Complex I activity was higher in IMPAD1-knockdown cells but reduced in IMPAD1-overexpressing cells (Fig. 7C and D), whereas the expression levels of IMPAD1 had no effect on Complex III activity (Supplementary Figs. 7A and B). We therefore determined whether Complex I mediates the expression of phosphorylated AMPK and HEY1. Indeed, treatment with rotentone, a Complex I inhibitor, increased the expression of pAMPK and HEY1 in IMPAD1-knockdown cells (Fig. 7E and Supplementary Fig. 7C). These data suggest that upregulated IMPAD1 enhances invasion by inhibiting Complex I activity, leading to reduced ROS production (Fig. 7F).

4. Discussion

The data presented here add to a growing body of literature indicating that metabolism in cancer cells contributes to the malignant phenotype, and is critical to signal transduction, tumorigenesis, and

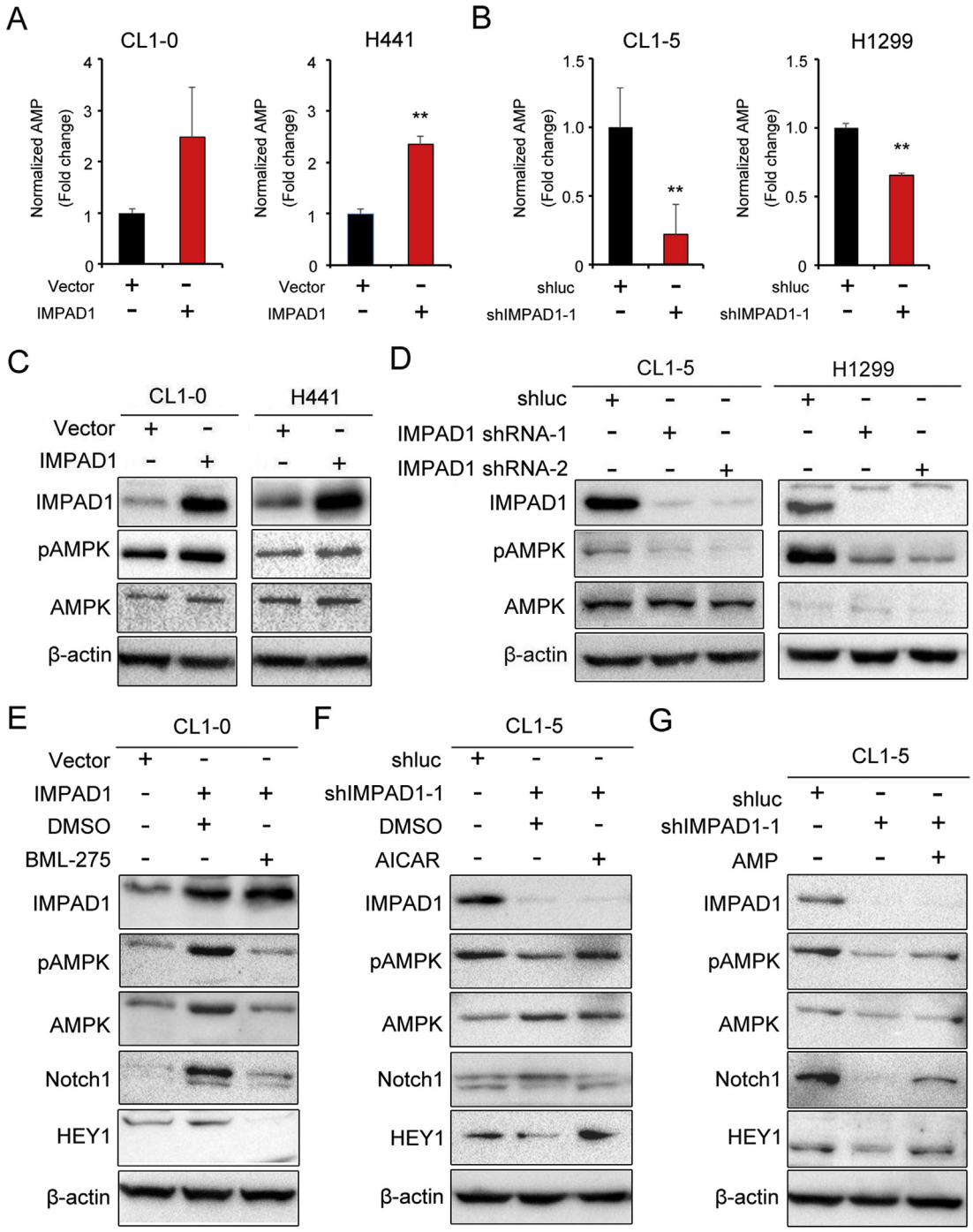

Fig. 4. IMPAD1 drives AMPK activation in lung cancer cells. (A) Changes in total AMP levels in the conditioned medium of CL1-0/IMPAD1 and H441/IMPAD1 cells. (B) Total AMP levels in the conditioned medium of CL1-5 and H1299 cells after IMPAD1 knockdown. (C) Expression of pAMPK in CL1-0 and H441 cells overexpressing IMPAD1 compared with the vector control. (D) Western blot analysis of pAMPK expression in CL1-5 and H1299 cells after infection with shluc or IMPAD1 shRNA. (E) CL1-0/IMPAD1 cells were treated with DMSO or 10 μM BML-275 (as AMPK kinase inhibitor) for 24 h and analyzed through Western blotting. (F) CL1-5/shIMPAD1 cells were treated with DMSO or 2 mM AICAR (as a AMPK activator) for 48 h and analyzed through Western blotting. (G) CL1-5/shIMPAD1 cells were treated with vehicle or AMP (38 nM) for 192 h and analyzed through Western blotting.

metastasis [30, 31]. IMPAD1 was identified from the highly invasive CL1-5 compared with the relatively non-invasive counterpart, CL1-0 [8]. We speculated the expression of IMPAD1 was correlated to invasion ability. Indeed, IMPAD1 was highly expressed in the more invasive CL1-5 and H1299 cells, but with low expression in the less invasive CL1-0 and H441 cells. IMPAD1 overexpression promoted the migration and invasion abilities in CL1-0 and H441 cells. Furthermore, IMPAD1 replenishment in the conditioned medium of CL1-5/shIMPAD1 increased the migration ability in CL1-0 and H441 cells. Together, these data suggest that intracellular and extracellular IMPAD1 may play an important role in lung cancer migration and invasion abilities. Specifically, this study indicates for the first time that the secretomic protein IMPAD1 is involved in lung cancer metastasis, both in patients' clinical data showing a significant association with lymph node metastasis, and *in vivo* with a de novo pathway indicating that IMPAD1 mediated metastasis through inhibition of mitochondrial Complex I activity to

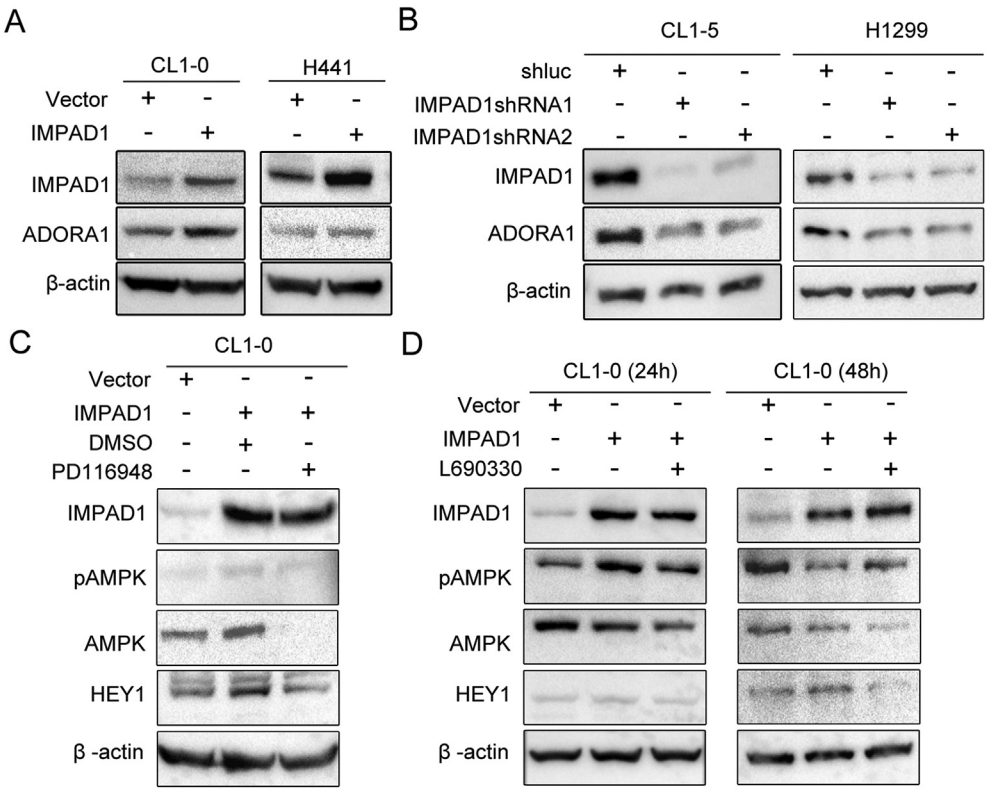

Fig. 5. IMPAD1-mediated ADORA1 activation is AMP-dependent in lung cancer cell lines. (A) ADORA1 expression and IMPAD1 expression were compared between CL1-0/IMPAD1 and H441/IMPAD1 cells and CL1-0/Vector and H441/Vector cells. (B) Expression of ADORA1 was compared between CL1-5 and H1299 cells with IMPAD1 knockdown and the shluc control. (C) CL1-0/IMPAD1 cells were treated with PD116,848 (10 μM, a ADORA1 antagonist) and assayed using Western blot with the indicated antibodies. (D) IMPAD1-overexpressing cells were treated with L690,330 (100 μM, as a IMPAD1 enzyme inhibitor) for 24 h and 48 h and were assayed using Western blotting with the indicated antibodies.

reduce ROS production, leading to AMPK phosphorylation, which in turn induced Notch1-mediated upregulation of HEY1.

The *IMPAD1* mutation is associated with chondrodysplasia and abnormal joint development through impairment of its enzyme activity [31], whilst loss of function in IMPAD1 leads to neonatal lethality in mice [32]. Other than IMPAD1, 3′(2′), 5′-bisphosphate nucleotidase 1 (BPNT1) may have a similar function in converting PAP to AMP in the cytoplasm [33]. IMPAD1 is a sulfotransferase that is normally located in golgi and converts PAP into AMP in human fibroblasts [32]. In the present study, we noted the upregulation of IMPAD1 and its mRNA levels in the CM of highly invasive CL1-5 lung cancer cells, suggesting that IMPAD1 is not only located in golgi but is also present in conditioned medium with undefined functions. IMPAD1 overexpression increased AMP levels in the CM of lung cancer cells, whereas decreased AMP levels were found in IMPAD1-knockdown cells. We noted that AMP replenishment restored the expression of pAMPK, Notch1, and HEY1 and migration ability in IMPAD1-knockdown lung cancer cells.

Under energy stress conditions, AMPK promotes tumor cell survival [13]. AMPK is a sensor of energy, and it can sense the change in AMP levels, even at very low levels [26,34,35]. AMP regulates AMPK by three complementary effects, including increased pAMPK by LKB1 [36], inhibition of AMPK dephosphorylation by protein phosphatase-2C alpha (PP2C alpha) [37], and allosteric activation [34]. AMPK activation also plays a critical role under energy stress conditions such as anchorage-independent growth. In particular, LKB1 appears to play a critical role under energy stress conditions such as anchorage-independent growth and solid tumor formation, promoting cell survival by AMPK activation and redox regulation [13]. LKB1-deficient cells are therefore resistant to oncogenic transformation and tumorigenesis [13,38]. LKB1 homozygous deletions and mutation are rare in somatic tumors, yet strikingly in NSCLC rates of 39% are reported, with up to 90% NSCLC showing loss of a single or both copies of the LKB1 locus [39]. A key unanswered question is therefore how LKB1 deficient NSCLC tumor cells can escape or bypass metabolic requirements during energy stress conditions [13]. Activation of AMPK restores ATP levels and promotes cell survival [13,40]. Overexpression of IMPAD1 may therefore provide one such an alternate pathway to AMPK activation in LKB1 deficient NSCLC (Fig. 7F). Although not the main focus of the present study, neither overexpression nor knockdown of IMPAD1 in lung cancer cells affected cell growth and ATP levels. Further work will be directed towards IMPAD1 overexpression and knockdown in LKB1 knockout models.

In the present study, we found that IMPAD1 overexpression increased pAMPK expression in lung cancer cells, whereas knockdown of IMPAD1 reduced pAMPK expression in lung cancer cells, by modulating AMP levels. Moreover, IMPAD1 expression increased AMP levels in the CM of lung cancer cells. AMP is also an ADORA1 agonist; treatment with an ADORA1 antagonist (PD116,948) significantly reduced the expression of pAMPK in IMPAD1-overexpressing cells. Similar to our results, Dada et al. also showed that the ADORA1 agonist 2-chloro-N^6-cyclopentyladenosine increased expression of pAMPK in alveolar epithelial cells [41]. Although we cannot exclude other pathways in AMP synthesis, this is the first study to demonstrate that IMPAD1 overexpression induces the upregulation of pAMPK by AMP through ADORA1.

Prior studies have indicated that Notch is involved in the regulation of glycolytic and oxidative metabolism, promoting glucose uptake and increasing OCR in T-cell acute lymphoblastic leukemia (T-ALL). Notch also activates AMPK to inhibit anabolic metabolism [42]. Similarly, our data showed that IMPAD1 overexpression upregulated the expression of Notch1 and reduced OCR in lung cancer cells). Furthermore, treatment with AMPK inhibitor BML-275 inhibited the expression of Notch1 and HEY1 in IMPAD1-overexpressing cells, whereas treatment with either the AMPK activator AICAR or with AMP restored Notch1 and HEY1 expression in IMPAD1-knockdown cells. Treatment with an IMPAD1 inhibitor (L690,330) reduced pAMPK expression in 24 h and HEY1 expression in 48 h in IMPAD1-overexpressing cells, whereas treatment with NAC (a free radical scavenger) restored pAMPK expression in 4h and HEY1 expression in 24h in IMPAD1-knockdown cells. This finding suggests that AMPK modulates Notch1 and HEY1 expression in IMPAD1-overexpressing cells.

AMPK can promote mitochondrial oxidative metabolism through

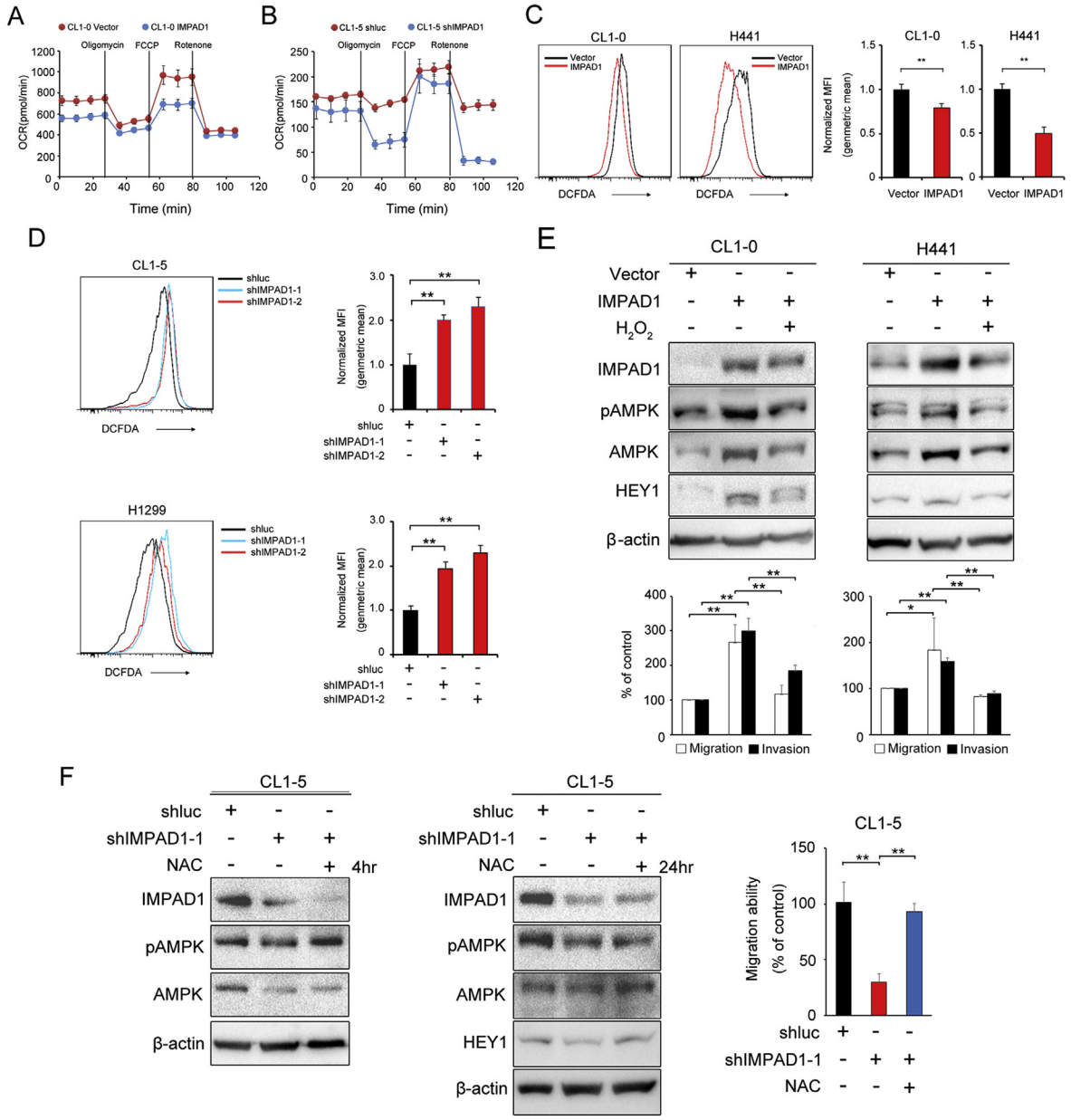

Fig. 6. Mitochondrial dysfunction in IMPAD1-overexpressing lung cancer cell lines. (A–B) Analysis of the oxygen consumption rate (OCR) in CL1-0/IMPAD1 cells (A) and CL1-5/shIMPAD1 cells (B). (C) Left, analysis of the ROS level by flow cytometry analysis of DCFDA in CL1-0/IMPAD1 and H441/IMPAD1 cells. Right, quantification of ROS level. Data are presented as mean ± SD. $^{**}P < 0.01$. (D) Left, analysis of the ROS level by flow cytometry analysis of DCFDA in CL1-5 and H1299 cells with IMPAD1 knockdown. Right, quantification of ROS level. Data are presented as the mean ± SD. $^{**}P < 0.01$. (E) IMPAD1-overexpressing cells were treated with H_2O_2 (80 μM) and assayed for Western blotting with the indicated antibodies (top) or invasion and migration using transwell chambers (bottom). Data are presented as the mean ± SD. $^{*}P < 0.05$; $^{**}P < 0.01$. (F) IMPAD1-knockdown cells were treated with NAC (10 mM) for 4 h and 24 h and assayed using Western blotting with the indicated antibodies (left) or migration using transwell chambers (right). Data are presented as the mean ± SD. $^{*}P < 0.05$; $^{**}P < 0.01$.

the modulation of Complex I activity [29,42]. The suppression of AMPK in T-ALL has been shown to reduce Complex I activity and OCR levels, leading to an increase in ROS levels. In T-ALL, AMPK is essential for maintaining mitochondria capacity [42]. Elizabeth et al. showed that treatment with H_2O_2 activated AMPK in C2C12 mouse myotubes [43]. In the present study, we showed that IMPAD1 overexpression inhibited Complex I activity and reduced ROS levels, leading to the increased expression of pAMPK in lung cancer lines. Treatment with NAC (a free radical scavenger) or rotentone (Complex I inhibitor) restored the expression of pAMPK in IMPAD1-knockdown cells. In contrast, treatment with H_2O_2 reduced pAMPK expression and inhibited migration/invasion abilities in IMPAD1-overexpressing cells. In agreement with our results, previous studies have shown that suppression of Complex I activity enhanced cell migration and invasion in breast cancer cell lines [44], and treatment with H_2O_2 reduced the expression of AMPK in a cardiomyocyte ischemia model [45]. Our data demonstrated that IMPAD1 inhibited mitochondrial Complex I activity, leading to decreased levels of ROS; thus increased pAMPK and HEY1 expression promoted migration and invasion abilities in lung cancer cells.

Recently Gamma secretase inhibitors (GSI), a class of small-molecule inhibitors that prevent the cleavage of γ-secretase substrates including the four Notch receptors and the five canonical transmembrane Notch ligands [46], have been explored in the context of NSCLC with the aim of sensitising tumors to chemotherapeutic agents such as paclitaxel [47]. However, somatic mutations in Notch are rare in NSCLC [48], perhaps accounting for the variable clinical efficacy of GSIs such

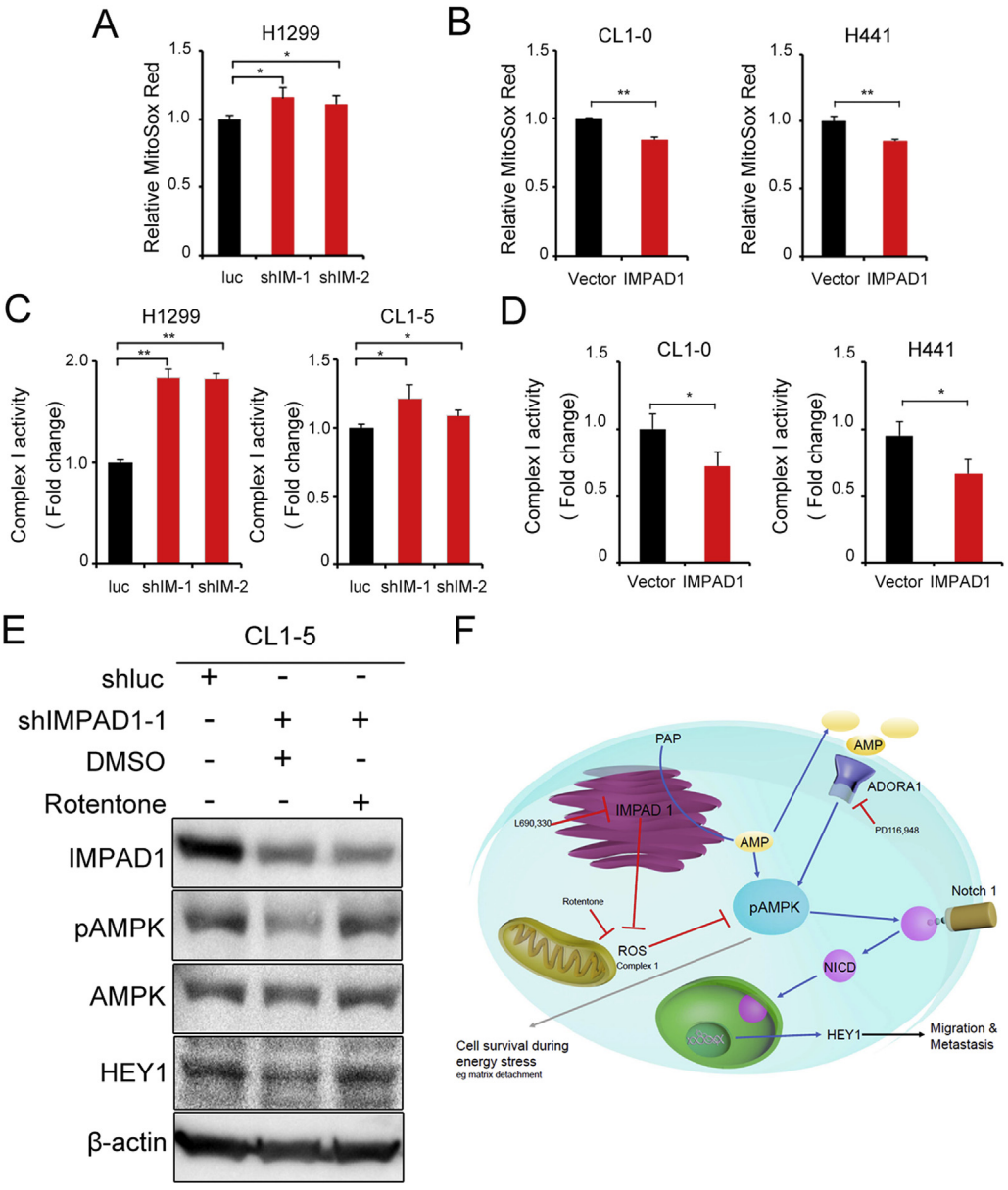

Fig. 7. IMPAD1 inhibits mitochondrial oxidative metabolism in lung cancer cells through the regulation of Complex I. (A–B) Analysis of ROS level by flow cytometry analysis of MitoSox in H1299 cells with IMPAD1 knockdown (A) as well as CL1-0 and H441 cells with IMPAD1 overexpression (B). Data are presented as the mean ± SD. *P < 0.05; **P < 0.01. (C–D) Analysis of Complex I enzyme activity in H1299 and CL1-5 cells with IMPAD1 knockdown (C) as well as CL1-0 and H441 cells with IMPAD1 overexpression (D). Data are presented as the mean ± SD. *P < 0.05; **P < 0.01. (E) IMPAD1-knockdown cells were treated with Retenone (0.5 μM, a mitochondrial electron transport inhibitor) and were assayed using Western blot analysis with the indicated antibodies. (F) Model showing that IMPAD1 inhibited Complex I activity, leading to reduce ROS levels and up-regulation of AMPK-Notch1-HEY1 signaling in lung cancer.

as AL101 [47,49]. Given that IMPAD1 is an upstream effector of Notch1, overexpression of IMPAD1 may provide a more suitable biomarker for GSI efficacy in NSCLC, and may allow therapeutic stratification of subsets of patients who are most likely to benefit. Further therapeutic targets in the IMPAD1-pAMPK-Notch1-HEY1 pathway include AMPK agonists, with the use of Mitochondrial complex I inhibitors such as metformin and phenformin [50,51], and more recently AMPK specific agonists such as D561-0775 in NSCLC showing promise in preclinical studies [52]. However, lack of efficacy in translational clinical studies of metformin with gefitinib, again points towards the need for a suitable biomarker for patient stratification [53].

The data presented here identified IMPAD1 for the first time as a clinically relevant metastasis-associated protein and prognostic marker in lung cancer patients. Significantly, we discovered a novel IMPAD1-pAMPK-Notch1-HEY1 pathway that promoted migration and invasion of lung cancer cells. IMPAD1 overexpression inhibited Complex I activity, reducing ROS production in lung cancer cell, promoting tumor cell invasion. Lastly, IMPAD1 may be critical in tumor metabolic reprogramming of NSCLC, providing an alternate route to activation of AMPK under energy stress conditions. Collectively our data suggests that IMPAD1 is a propitious metabolic therapeutic target and a novel biomarker in lung cancer metastasis that may allow stratification of emerging therapies such as GSIs.

Author contributions statement

The authors contributed in the following way: design and write the manuscripts: Y.-F.Y and S.-S.F. Y; provide materials: M.H, Y–Y W and S.-S.F. Y; perform experiments: Y.-F. Y, Y.-C.C, Y.-H. J and T-C. L; interpret data: Y.-F. Y, Y.-C. L, S.L, Y.-C H, M.H and S.-S.F·Y.

Declaration of competing interest

No potential conflicts of interest were disclosed.

Acknowledgments

This work was supported by grants from the National Science Council (MOST 106-2314-B-037-005-MY2, MOST108-2320-B-075B-005, and MOST107-2314-B-037-097-MY2), Kaohsiung Medical University Hospital (KMUH107-7R91 and KMUH107-7R36), and

NCTU-KMU joint grant (NCTUKMU108-DR-01).

Appendix A. Supplementary data

Supplementary data to this article can be found online at https://doi.org/10.1016/j.canlet.2020.04.025.

References

[1] D.M. Parkin, F. Bray, J. Ferlay, P. Pisani, Global cancer statistics, CA Cancer J Clin 55 (2005) (2002) 74–108.
[2] D.C. Ihde, Chemotherapy of lung cancer, N. Engl. J. Med. 327 (1992) 1434–1441.
[3] P.C. Hoffman, A.M. Mauer, E.E. Vokes, Lung cancer, Lancet 355 (2000) 479–485.
[4] D.M. Parkin, Global cancer statistics in the year 2000, the Lancet, Oncology 2 (2001) 533–543.
[5] A. Spira, D.S. Ettinger, Multidisciplinary management of lung cancer, N. Engl. J. Med. 350 (2004) 379–392.
[6] R.S. Herbst, J.V. Heymach, S.M. Lippman, Lung cancer, N. Engl. J. Med. 359 (2008) 1367–1380.
[7] L.A. Liotta, E.C. Kohn, The microenvironment of the tumour-host interface, Nature 411 (2001) 375–379.
[8] Y.H. Chang, S.H. Lee, I.C. Liao, S.H. Huang, H.C. Cheng, P.C. Liao, Secretomic analysis identifies alpha-1 antitrypsin (A1AT) as a required protein in cancer cell migration, invasion, and pericellular fibronectin assembly for facilitating lung colonization of lung adenocarcinoma cells, Mol. Cell. Proteomics 11 (2012) 1320–1339.
[9] M.C. Wang, Y.H. Chang, C.C. Wu, Y.C. Tyan, H.C. Chang, Y.G. Goan, W.W. Lai, P.N. Cheng, P.C. Liao, Alpha-actinin 4 is associated with cancer cell motility and is a potential biomarker in non-small cell lung cancer, J. Thorac. Oncol. : official publication of the International Association for the Study of Lung Cancer 10 (2015) 286–301.
[10] M.W. Volmer, K. Stuhler, M. Zapatka, A. Schoneck, S. Klein-Scory, W. Schmiegel, H.E. Meyer, I. Schwarte-Waldhoff, Differential proteome analysis of conditioned media to detect Smad4 regulated secreted biomarkers in colon cancer, Proteomics 5 (2005) 2587–2601.
[11] R.J. Simpson, J.W. Lim, R.L. Moritz, S. Mathivanan, Exosomes: proteomic insights and diagnostic potential, Expet Rev. Proteonomics 6 (2009) 267–283.
[12] S. Mathivanan, J.W. Lim, B.J. Tauro, H. Ji, R.L. Moritz, R.J. Simpson, Proteomics analysis of A33 immunoaffinity-purified exosomes released from the human colon tumor cell line LIM1215 reveals a tissue-specific protein signature, Mol. Cell. Proteomics : MCP 9 (2010) 197–208.
[13] S.M. Jeon, N.S. Chandel, N. Hay, AMPK regulates NADPH homeostasis to promote tumour cell survival during energy stress, Nature 485 (2012) 661–665.
[14] S. Vyas, E. Zaganjor, M.C. Haigis, Mitochondria and cancer, Cell 166 (2016) 555–566.
[15] M.P. Murphy, How mitochondria produce reactive oxygen species, Biochem. J. 417 (2009) 1–13.
[16] L.B. Sullivan, N.S. Chandel, Mitochondrial reactive oxygen species and cancer, Canc. Metabol. 2 (2014) 17.
[17] K.A. Conklin, Chemotherapy-associated oxidative stress: impact on chemotherapeutic effectiveness, Integr. Canc. Ther. 3 (2004) 294–300.
[18] C. Gorrini, I.S. Harris, T.W. Mak, Modulation of oxidative stress as an anticancer strategy, Nat. Rev. Drug Discov. 12 (2013) 931–947.
[19] B. Gyorffy, P. Surowiak, J. Budczies, A. Lanczky, Online survival analysis software to assess the prognostic value of biomarkers using transcriptomic data in non-small-cell lung cancer, PloS One 8 (2013) e82241.
[20] Y.F. Yang, Y.C. Lee, S. Lo, Y.N. Chung, Y.C. Hsieh, W.C. Chiu, S.F. Yuan, A positive feedback loop of IL-17B-IL-17RB activates ERK/beta-catenin to promote lung cancer metastasis, Canc. Lett. 422 (2018) 44–55.
[21] H. Yabushita, M. Shimazu, H. Yamada, K. Sawaguchi, M. Noguchi, M. Nakanishi, M. Kawai, Occult lymph node metastases detected by cytokeratin immunohistochemistry predict recurrence in node-negative endometrial cancer, Gynecol. Oncol. 80 (2001) 139–144.
[22] B. Zhang, J. Wang, W. Liu, Y. Yin, D. Qian, H. Zhang, B. Shi, C. Li, J. Zhu, L. Zhang, L. Gao, C. Wang, Cytokeratin 18 knockdown decreases cell migration and increases chemosensitivity in non-small cell lung cancer, J. Canc. Res. Clin. Oncol. 142 (2016) 2479–2487.
[23] T. Fukusumi, T.W. Guo, A. Sakai, M. Ando, S. Ren, S. Haft, C. Liu, P. Amornphimoltham, J.S. Gutkind, J.A. Califano, The NOTCH4-HEY1 pathway induces epithelial-mesenchymal transition in head and neck squamous cell carcinoma, Clin. Canc. Res. 24 (2018) 619–633.
[24] T. Iso, V. Sartorelli, G. Chung, T. Shichinohe, L. Kedes, Y. Hamamori, HERP, a new primary target of Notch regulated by ligand binding, Mol. Cell Biol. 21 (2001) 6071–6079.
[25] T. Iso, G. Chung, Y. Hamamori, L. Kedes, HERP1 is a cell type-specific primary target of Notch, J. Biol. Chem. 277 (2002) 6598–6607.
[26] D.G. Hardie, AMPK–sensing energy while talking to other signaling pathways, Cell Metabol. 20 (2014) 939–952.
[27] Z. Lin, P. Yin, S. Reierstad, M. O'Halloran, V.J. Coon, E.K. Pearson, G.M. Mutlu, S.E. Bulun, Adenosine A1 receptor, a target and regulator of estrogen receptoralpha action, mediates the proliferative effects of estradiol in breast cancer, Oncogene 29 (2010) 1114–1122.
[28] J.E. Rittiner, I. Korboukh, E.A. Hull-Ryde, J. Jin, W.P. Janzen, S.V. Frye, M.J. Zylka, AMP is an adenosine A1 receptor agonist, J. Biol. Chem. 287 (2012) 5301–5309.
[29] L. Lantier, J. Fentz, R. Mounier, J. Leclerc, J.T. Treebak, C. Pehmoller, N. Sanz, I. Sakakibara, E. Saint-Amand, S. Rimbaud, P. Maire, A. Marette, R. Ventura-Clapier, A. Ferry, J.F. Wojtaszewski, M. Foretz, B. Viollet, AMPK controls exercise endurance, mitochondrial oxidative capacity, and skeletal muscle integrity, Faseb. J. 28 (2014) 3211–3224.
[30] D.B. Zorov, M. Juhaszova, S.J. Sollott, Mitochondrial reactive oxygen species (ROS) and ROS-induced ROS release, Physiol. Rev. 94 (2014) 909–950.
[31] L.E. Vissers, E. Lausch, S. Unger, A.B. Campos-Xavier, C. Gilissen, A. Rossi, M. Del Rosario, H. Venselaar, U. Knoll, S. Nampoothiri, M. Nair, J. Spranger, H.G. Brunner, L. Bonafe, J.A. Veltman, B. Zabel, A. Superti-Furga, Chondrodysplasia and abnormal joint development associated with mutations in IMPAD1, encoding the Golgi-resident nucleotide phosphatase, gPAPP, Am. J. Hum. Genet. 88 (2011) 608–615.
[32] J.P. Frederick, A.T. Tafari, S.M. Wu, L.C. Megosh, S.T. Chiou, R.P. Irving, J.D. York, A role for a lithium-inhibited Golgi nucleotidase in skeletal development and sulfation, Proc. Natl. Acad. Sci. U. S. A. 105 (2008) 11605–11612.
[33] B.D. Spiegelberg, J.P. Xiong, J.J. Smith, R.F. Gu, J.D. York, Cloning and characterization of a mammalian lithium-sensitive bisphosphate 3'-nucleotidase inhibited by inositol 1,4-bisphosphate, J. Biol. Chem. 274 (1999) 13619–13628.
[34] G.J. Gowans, S.A. Hawley, F.A. Ross, D.G. Hardie, AMP is a true physiological regulator of AMP-activated protein kinase by both allosteric activation and enhancing net phosphorylation, Cell Metabol. 18 (2013) 556–566.
[35] X. Li, L. Wang, X.E. Zhou, J. Ke, P.W. de Waal, X. Gu, M.H. Tan, D. Wang, D. Wu, H.E. Xu, K. Melcher, Structural basis of AMPK regulation by adenine nucleotides and glycogen, Cell Res. 25 (2015) 50–66.
[36] B. Faubert, G. Boily, S. Izreig, T. Griss, B. Samborska, Z. Dong, F. Dupuy, C. Chambers, B.J. Fuerth, B. Viollet, O.A. Mamer, D. Avizonis, R.J. DeBerardinis, P.M. Siegel, R.G. Jones, AMPK is a negative regulator of the Warburg effect and suppresses tumor growth in vivo, Cell Metabol. 17 (2013) 113–124.
[37] S.P. Davies, N.R. Helps, P.T. Cohen, D.G. Hardie, 5'-AMP inhibits dephosphorylation, as well as promoting phosphorylation, of the AMP-activated protein kinase. Studies using bacterially expressed human protein phosphatase-2C alpha and native bovine protein phosphatase-2AC, FEBS Lett. 377 (1995) 421–425.
[38] N. Bardeesy, M. Sinha, A.F. Hezel, S. Signoretti, N.A. Hathaway, N.E. Sharpless, M. Loda, D.R. Carrasco, R.A. DePinho, Loss of the Lkb1 tumour suppressor provokes intestinal polyposis but resistance to transformation, Nature 419 (2002) 162–167.
[39] R.K. Gill, S.H. Yang, D. Meerzaman, L.E. Mechanic, E.D. Bowman, H.S. Jeon, S. Roy Chowdhuri, A. Shakoori, T. Dracheva, K.M. Hong, J. Fukuoka, J.H. Zhang, C.C. Harris, J. Jen, Frequent homozygous deletion of the LKB1/STK11 gene in non-small cell lung cancer, Oncogene 30 (2011) 3784–3791.
[40] K. Inoki, T. Zhu, K.L. Guan, TSC2 mediates cellular energy response to control cell growth and survival, Cell 115 (2003) 577–590.
[41] L. Dada, A.R. Gonzalez, D. Urich, S. Soberanes, T.S. Manghi, S.E. Chiarella, N.S. Chandel, G.R. Budinger, G.M. Mutlu, Alcohol worsens acute lung injury by inhibiting alveolar sodium transport through the adenosine A1 receptor, PloS One 7 (2012) e30448.
[42] R.J. Kishton, C.E. Barnes, A.G. Nichols, S. Cohen, V.A. Gerriets, P.J. Siska, A.N. Macintyre, P. Goraksha-Hicks, A.A. de Cubas, T. Liu, M.O. Warmoes, E.D. Abel, A.E. Yeoh, T.R. Gershon, W.K. Rathmell, K.L. Richards, J.W. Locasale, J.C. Rathmell, AMPK is essential to balance glycolysis and mitochondrial metabolism to control T-ALL cell stress and survival, Cell Metabol. 23 (2016) 649–662.
[43] E.C. Hinchy, A.V. Gruszczyk, R. Willows, N. Navaratnam, A.R. Hall, G. Bates, T.P. Bright, T. Krieg, D. Carling, M.P. Murphy, Mitochondria-derived ROS activate AMP-activated protein kinase (AMPK) indirectly, J. Biol. Chem. 293 (2018) 17208–17217.
[44] X. He, A. Zhou, H. Lu, Y. Chen, G. Huang, X. Yue, P. Zhao, Y. Wu, Suppression of mitochondrial complex I influences cell metastatic properties, PloS One 8 (2013) e61677.
[45] D. Shao, S. Oka, T. Liu, P. Zhai, T. Ago, S. Sciarretta, H. Li, J. Sadoshima, A redox-dependent mechanism for regulation of AMPK activation by Thioredoxin1 during energy starvation, Cell Metabol. 19 (2014) 232–245.
[46] K.M. Capaccione, S.R. Pine, The Notch signaling pathway as a mediator of tumor survival, Carcinogenesis 34 (2013) 1420–1430.
[47] K.M. Morgan, B.S. Fischer, F.Y. Lee, J.J. Shah, J.R. Bertino, J. Rosenfeld, A. Singh, H. Khiabanian, S.R. Pine, Gamma secretase inhibition by BMS-906024 enhances efficacy of paclitaxel in lung adenocarcinoma, Mol. Canc. Therapeut. 16 (2017) 2759–2769.
[48] N. Cancer, Genome Atlas Research, Comprehensive molecular profiling of lung adenocarcinoma, Nature 511 (2014) 543–550.
[49] S.R. Pine, Rethinking gamma-secretase inhibitors for treatment of non-small-cell lung cancer: is Notch the target? Clin. Canc. Res. 24 (2018) 6136–6141.
[50] D.B. Shackelford, R.J. Shaw, The LKB1-AMPK pathway: metabolism and growth control in tumour suppression, Nat. Rev. Canc. 9 (2009) 563–575.
[51] H. Chen, C. Lin, C. Lu, Y. Wang, R. Han, L. Li, S. Hao, Y. He, Metformin-sensitized NSCLC cells to osimertinib via AMPK-dependent autophagy inhibition, Clin. Res. J 12 (2019) 781–790.
[52] X. Chen, Y. Chen, J. Jiang, L. Wu, S. Yin, X. Miao, R.J. Swanson, S. Zheng, Nanopulse stimulation (NPS) ablate tumors and inhibit lung metastasis on both canine spontaneous osteosarcoma and murine transplanted hepatocellular carcinoma with high metastatic potential, Oncotarget 8 (2017) 44032–44039.
[53] L. Li, L. Jiang, Y. Wang, Y. Zhao, X.J. Zhang, G. Wu, X. Zhou, J. Sun, J. Bai, B. Ren, K. Tian, Z. Xu, H.L. Xiao, Q. Zhou, R. Han, H. Chen, H. Wang, Z. Yang, C. Gao, S. Cai, Y. He, Combination of metformin and gefitinib as first-line therapy for nondiabetic advanced NSCLC patients with EGFR mutations: a randomized, double-blind phase II trial, Clin. Canc. Res. 23 (2019) 6967–6975.